EASR

Engineering and Applied Science Research

https://www.tci-thaijo.org/index.php/easr/index

Published by the Faculty of Engineering, Khon Kaen University, Thailand

Drying of tamarind foam-mats using far-infrared radiation combined with a belt conveyor system: Drying kinetics, quality attributes, and mathematical modeling

Poomjai Sa-adchom*

Department of Mechanical Engineering, Faculty of Engineering, Rajamangala University of Technology Lanna, Tak 63000, Thailand

Received 28 August 2023
Revised 6 October 2023
Accepted 9 October 2023

Abstract

The study aimed to evaluate the effects of far-infrared radiation (FIR) power level and the thickness of tamarind foam-mats (TFMs) on changes in moisture content during the drying process. This process involved the use of far-infrared radiation, combined with a belt conveyor system (FIR+BCS), to dry the TFMs. Specific energy consumption (SEC) and quality attributes of tamarind powder, such as color and dissolution time, were examined. The study also investigated a mathematical model to describe the suitable drying characteristics of TFMs. In the experiment, cylindrical TFMs with a diameter of 5 cm and thicknesses of 3 and 6 mm were dried using FIR+BCS at FIR power levels of 400, 500, and 600 W until the moisture content of the TFMs was reduced to less than 13% w.b. Based on the experimental results, it was found that higher FIR power levels led to more rapid decreases in moisture content in TFMs, lower SEC, and quicker dissolution of tamarind powder in water, compared to lower FIR power levels. The 3 mm thick TFMs exhibited faster moisture content reduction, lower SEC, and more rapid dissolution of tamarind powder in water than the 6 mm thick ones. In addition, tamarind powder produced from 6 mm thick TFMs had higher lightness (L^* value) and yellowness (b^* value), but lower redness (a^* value) than those of 3 mm thick TFMs. However, tamarind powder produced from TFMs with FIR power levels of 400, 500, and 600 W were not significantly different in color values (L^*, a^*, and b^* values). Among the seven mathematical models, the Midilli et al. model satisfactorily described the drying kinetics of TFMs, with an R^2 value of 0.993269, an RMSE of 0.005117, and a χ^2 value of 0.000321. The effective moisture diffusivity values of TFMs ranged from 9.41×10^{-10} to 2.33×10^{-9} m^2/s.

Keywords: Belt conveyor system, Drying kinetics, Far-infrared radiation, Mathematical modeling, Quality attributes, Tamarind foam-mats

1. Introduction

Tamarind (*Tamarindus indica* L.) is an evergreen fruit-bearing tree belonging to the Fabaceae family [1], widely distributed across tropical regions. Its pods contain a pulp that is rich in vitamins, minerals, dietary fiber, and bioactive compounds such as polyphenols and flavonoids [2]. The unique blend of sweet and sour flavors makes tamarind a versatile ingredient in culinary practices and a popular choice for various food products, including beverages, chutneys, sauces, and confectioneries. Despite its numerous benefits, tamarind's high moisture content makes it susceptible to microbial degradation and enzymatic reactions, leading to rapid deterioration. Conventional drying methods like sun drying and hot air drying have been employed to reduce the moisture content, but these methods often result in undesirable quality attributes due to prolonged drying time and potential loss of volatile compounds [3]. The foam-mat drying technique, introduced as an alternative to overcome these limitations, entails forming a stable foam from tamarind pulp and drying it to obtain a light and porous foam-mats product, which exhibits improved rehydration properties and prolonged shelf-life [4].

Foam-mat drying is a relatively new and innovative approach to food drying, which has gained considerable attention in recent years. It involves generating a stable foam from food puree or extract by incorporating a foaming agent, followed by drying the foam to obtain a lightweight and porous solid product. The technique is particularly useful for moisture-sensitive products, as it significantly reduces drying time and enhances the preservation of bioactive compounds [5], flavor, and color [6]. Additionally, foam-mat drying offers several other benefits, such as ease of handling, reduced transportation costs due to the lightweight nature of the product, and improved reconstitution properties during subsequent use. Foam-mat drying has also been explored for various products, including lime juice [7], papaya [8], cantaloupe [9], mango [10], and tamarind [11, 12]. In a study focused on tamarind foam-mat drying, Silva et al. [11] examined the influence of drying temperature on the drying kinetics of tamarind foam-mats (TFMs) and developed a mathematical model for its drying process. Their investigation revealed that when drying TFMs with a 5 mm thickness using hot air temperatures of 50, 60, 70, and 80ºC, the corresponding drying times were 4.3, 3.4, 3.0, and 2.5 h, respectively. Additionally, their findings indicated that the Midilli et al. model provided the most accurate representation of the drying curve behavior. According to a study by Ekpong et al. [12], it was suggested that drying TFMs using hot air at temperatures below 55°C caused the foam-mats structure

*Corresponding author.
Email address: poomjai.s@gmail.com
doi: 10.14456/easr.2023.60

to collapse, rendering the finished product unacceptable as a powder. On the other hand, drying TFMs using hot air at a temperature of 70°C resulted in a better pore structure and improved emulsion stability of the tamarind foam. This process prevented collapse and produced a highly acceptable powder. Based on the research mentioned above, it was discovered that drying TFMs was conducted using hot air. The introduction of far-infrared radiation as the heat source has garnered significant attention for enhancing the drying process.

Far-infrared radiation (FIR) drying is a process that utilizes the electromagnetic spectrum in the far-infrared range (typically between 3 and 1,000 μm [13]) to efficiently remove moisture from various materials, including food products, coatings, and textiles. This method operates by emitting electromagnetic waves that penetrate the material's surface, causing water molecules to vibrate and release moisture in the form of vapor. One significant advantage of FIR drying is its efficiency in uniformly and rapidly removing moisture while preserving the quality, color, and flavor of the materials being dried. Furthermore, it provides precise temperature control, reduces drying time, and is regarded as energy-efficient, thus presenting a cost-effective alternative to conventional drying methods [14]. FIR is also known to exhibit selectivity in heating, wherein it primarily targets the moisture content of the food matrix, leaving the structure and integrity of the food largely unaffected [15]. This characteristic makes it particularly suitable for drying high-moisture products, such as tamarind foam-mats (TFMs), where preserving the nutritional and sensory attributes is of paramount importance. A research study conducted by Sa-adchom et al. [16] investigated the effect of drying temperature on the drying kinetics of TFMs undergoing FIR drying. The study also aimed to determine the specific energy consumption (SEC) and the color of dried TFMs. They observed that when using drying temperatures of 60, 70, and 80°C, the moisture content of TFMs decreased from 80% w.b. to below 13% w.b. within 120, 100, and 80 min, respectively. The SEC and redness (a^* value) of dried TFMs increased with increasing temperature, while the lightness (L^* value) and yellowness (b^* value) of dried TFMs decreased with increasing temperature. According to a study by Salehi and Satorabi [17], the effects of different infrared (IR) power levels (150, 250, and 375 W) on the drying kinetics, moisture content, and effective moisture diffusivity (D_{eff}) of apple slices coated with basil seed and xanthan gums during IR drying were examined. They found that as the IR power levels increased, the drying times and moisture contents of the apple slices decreased, while the D_{eff} values increased. Additionally, the Page model was found to be the most suitable for depicting the kinetic behavior, providing an accurate description of the IR drying behavior of the apple slices.

In conventional foam-mat drying processes, the drying rate and overall efficiency are limited by the static drying environment, which often leads to uneven drying and longer processing times. To address these challenges, the integration of a belt conveyor system in the foam-mat drying setup offers a dynamic and continuous drying environment. A belt conveyor system allows for a controlled and uniform movement of the foam-mats product through the drying chamber, enabling consistent exposure to far-infrared radiation. As a result, the drying process becomes more efficient, ensuring homogeneity in moisture removal and reducing the risk of over-drying or under-drying. This integration optimizes the drying conditions, leading to improved product quality and reduced processing time.

Although many studies have been conducted on the drying of tamarind foam-mats (TFMs) using hot air and far-infrared radiation (FIR), there has been no research on the effect of FIR power level on the drying kinetics and quality attributes of tamarind powder. Furthermore, the drying of TFMs using FIR combined with a belt conveyor system has not been previously investigated. Therefore, the objective of this study was to evaluate the effects of FIR power level (400, 500, and 600 W) and the thickness of tamarind foam-mats (3 and 6 mm) on changes in moisture content during the drying process using FIR combined with a belt conveyor system. The study also aimed to determine the specific energy consumption (SEC) and assess the quality attributes of tamarind powder, particularly in terms of color and dissolution time. Seven mathematical models were considered to describe the drying kinetics of TFMs. The performance of these models was investigated by comparing between the observed and predicted moisture ratios using the coefficient of determination (R^2), root mean square error (RMSE) and reduced chi-square (χ^2). By delving into this innovative approach, the research strives to contribute to the advancement of food processing technologies and offer valuable insights into the potential benefits of incorporating advanced drying techniques for enhancing the preservation of tropical fruits like tamarind. Ultimately, this research may pave the way for sustainable and efficient drying methods, promoting food security, reducing post-harvest losses, and ensuring the availability of nutritious and flavorful products to consumers worldwide.

The research hypothesis for this study posited that variations in the far-infrared radiation (FIR) power level and the thickness of tamarind foam-mats would significantly impact the drying kinetics, specific energy consumption, as well as the quality attributes, including color and dissolution time, of tamarind powder. The reasons for formulating this hypothesis were rooted in the potential of FIR to enhance drying efficiency and preserve the quality attributes of agricultural products [17]. The thickness of the foam-mats was also intrinsically linked to drying time and energy consumption [10], making its investigation in combination with FIR essential. Additionally, the study aimed to develop a mathematical model that could accurately describe the drying behavior and determine the effective moisture diffusivity under different drying conditions.

2. Materials and methods

2.1 Experimental set-up

A schematic diagram of the far-infrared dryer combined with a belt conveyor system used in this study is shown in Figure 1. The system consisted of several components: a drying chamber measuring 0.5×0.5×1.2 m (width × height × length) (No.1), four ceramic far-infrared heaters (No. 2), each with a heating area of 6×24.5 cm (width × length) and an electrical power level of 400 W (Infrapara, model A-1-400, Thailand), a 304 stainless steel mesh belt conveyor system measuring 0.3×1 m (width × length) (No.3), a 100 W gear motor (Mitsubishi, model GM-S, Japan) (No.4), a motor speed controller (Reckon, model RK-2000, Thailand) (No.5), a slide voltage regulator (Union, model TDGC2-series, Thailand) (No.6), a digital clamp meter (Sanwa, model DCM60L, Japan) (No.7), and an electric meter (Dai-ichi, model DD28, Thailand) (No.8).

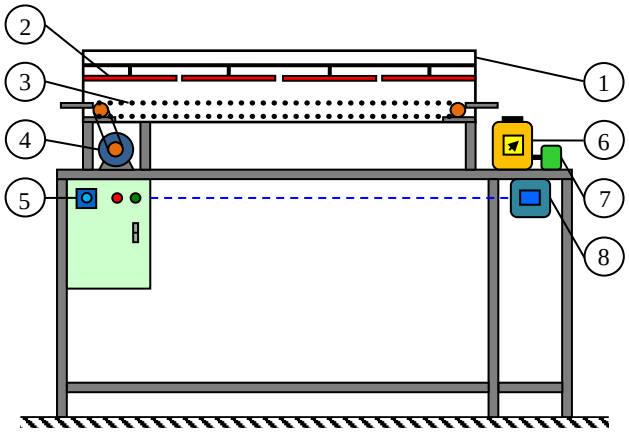

Figure 1 A schematic diagram of the far-infrared dryer combined with a belt conveyor system: (1) drying chamber, (2) far-infrared heaters, (3) conveyor belt, (4) gear motor, (5) motor speed controller, (6) slide voltage regulator, (7) digital clamp meter, and (8) electric meter

The working principle of this dryer involved the product moving along the conveyor belt at a speed of 4 cm/min into the drying chamber. Far-infrared heaters, positioned on the top wall of the drying chamber, transferred heat by radiating it onto the product using far-infrared radiation at power levels of 400, 500, and 600 W (The far-infrared heaters were equipped with four tubes. When operating at a power level of 400 W for far-infrared radiation, each tube consumed 100 W. At 500 W, each tube consumed 125 W; and at 600 W, each tube consumed 150 W). The distance between the far-infrared heaters and the product was 10 cm. To minimize heat loss to the surroundings, the drying chamber was insulated with 12.5 cm thick glass wool.

2.2 Sample preparation

2.2.1 Preparation of tamarind pulp

The sour tamarind, compressed into pulp form and stored in a cold room at a temperature of 5°C for 15 days, was purchased from a store in the Mueang District of Tak Province, Thailand. To prepare the tamarind pulp, the compressed tamarind was combined with water in a 1:2 weight ratio [16] and then blended. Afterward, the tamarind pulp was manually separated from the seed membrane.

2.2.2 Preparation of the mixture

The mixture for tamarind foam-mats production was formulated based on the method proposed by Sa-adchom et al. [16]. The ingredients used were 340 g of tamarind pulp, 17 g of maltodextrin DE10 (WGC Co., Ltd., Thailand), and 104.25 g of hydroxypropyl methylcellulose (HPMC) gel. To prepare the 104.25 g of HPMC gel, 4.25 g of powdered HPMC E4M (Modernist Pantry, LLC, USA) was added to 100 g of hot distilled water (at 90°C) in a 250 ml beaker. The mixture was stirred using a glass stick until it formed a smooth, clear, and non-cloudy gel.

2.2.3 Preparation of tamarind foam-mats

Tamarind pulp (340 g) was mixed with maltodextrin (17 g) using a mixer machine (Mixer, model B5, Thailand) equipped with a basket-shaped beater head. The mixture was stirred at a maximum speed of 147 rpm until a homogeneous mixture was obtained. Subsequently, 104.25 g of HPMC gel was added to the mixture, and the blender was operated within the mixer machine for 10 min to produce the tamarind foam. Finally, the tamarind foam was placed in cylindrical aluminum foil shapes with a diameter of 5 cm and heights of 3 mm and 6 mm. It should be noted that a tamarind foam-mat in aluminum foil with a thickness of 3 mm had a mass of 6 g, while a tamarind foam-mat in aluminum foil with a thickness of 6 mm had a mass of 12 g.

2.3 Methods

Tamarind foam-mats (TFMs) with an initial moisture content of approximately 76% w.b. and thicknesses of 3 and 6 mm were dried using a far-infrared dryer combined with a belt conveyor system at far-infrared radiation (FIR) power levels of 400, 500, and 600 W. The drying process continued until the final moisture content of the TFMs was reduced to less than 13% w.b. [16]. It should be noted that in each experiment, 24 pieces of 3 mm thick TFMs (with a total mass of 144 g) were used for drying. Similarly, for drying 6 mm thick TFMs, 24 pieces (with a total mass of 288 g) were used. Subsequently, the dried TFMs were ground into tamarind powder using a grinder (OOTD, model FG500Y, China) with a capacity of 500 g for a duration of 3 min.

The moisture content of tamarind foam-mat samples was assessed by employing a moisture analyzer (Ohaus model MB23, Germany) with a precision of 0.01 g, at different drying durations (0, 15, 30, 45, 60, ... min). The trials were replicated three times, and the mean values accompanied by their corresponding standard deviations were reported.

2.4 Specific energy consumption

The measure of specific energy consumption (SEC) in the drying process, which utilized a combination of far-infrared radiation and a belt conveyor system (FIR+BCS), referred to the energy needed to extract a given mass of water from the product being dried. This critical parameter played a significant role in assessing the dryer's energy efficiency and fine-tuning its operational performance. SEC could be determined using Eq. (1) with the following formula [18]:

$$\mathrm{SEC} = \frac{3.6\mathrm{Q}}{\mathrm{m_w}} \quad (1)$$

where SEC was the specific energy consumption (MJ/kg_{water}), Q was the energy provided during the drying process (kWh), m_w was the mass of water evaporated during the drying process (kg_{water}), and 3.6 was the factor for converting kWh to MJ. All the experiments were performed in triplicate.

2.5 Color

In the study, a colorimeter (Konica Minolta, model CR-10 Plus, Japan) was used to measure the surface colors of samples both before and after drying, as well as the colors of powdered samples. A standardized D65 light source was employed as the illuminant for this analysis, and the observation angle was set at 10°. The measurements were taken with an 8 mm aperture size in conjunction with a closed cone setup. Furthermore, the mass of the sample used to assess the color was approximately 50 g. The L^*, a^*, b^* color system was set up on the colorimeter, where L^* indicated lightness, a^* indicated the presence of redness (+) or greenness (-), and b^* indicated the presence of yellowness (+) or blueness (-). Before each color measurement, the colorimeter was calibrated using a standard white tile. The color difference (ΔE) for the samples was calculated from the collected data using the following equation [19]:

$$\Delta E = \sqrt{(\Delta L)^2 + (\Delta a)^2 + (\Delta b)^2} \quad (2)$$

where $\Delta L = L^* - L_0^*$, $\Delta a = a^* - a_0^*$, and $\Delta b = b^* - b_0^*$. The color of the samples before drying was denoted by the color parameters L_0^*, a_0^*, and b_0^*. These pre-drying samples served as the reference material. A larger ΔE value signified a more noticeable deviation in color from this reference. In each experiment, three samples were taken, and their surfaces were analyzed. The average color measurement for each experiment was then recorded.

2.6 Dissolution time

The dissolution time of tamarind powder was determined by adding 10 g of tamarind powder to 250 ml of distilled water at 26°C [20]. The mixture was agitated in a 500 ml glass beaker using a magnetic stirrer (HANNA, model HI304N, USA) at 1,000 rpm, with a stirring bar measuring 8×25 mm (width × length). The time taken for the material to dissolve completely was recorded. Each treatment was replicated three times, and the average of the dissolution time values was reported.

2.7 Mathematical modeling of drying

The moisture ratio (MR) was calculated using Eq. (3) based on the data obtained from the drying experiment, as presented below:

$$\mathrm{MR} = \frac{\mathrm{M_t} - \mathrm{M_e}}{\mathrm{M_0} - \mathrm{M_e}} \quad (3)$$

where MR was the moisture ratio (-), M_t was the moisture content at any time of drying (kg_{water}/kg_{solid}), M_0 was the initial moisture content (kg_{water}/kg_{solid}), and M_e was equilibrium moisture content (kg_{water}/kg_{solid}). Because the samples were not dried under consistent conditions of relative humidity and temperature, the M_e values were notably less compared to M_t or M_0 [21]. This led to the expression of the moisture ratio as M_t/M_0.

Seven mathematical drying models, as shown in Table 1, were examined to find the best fit for describing the drying process of tamarind foam-mats. Each model's effectiveness was assessed through three statistical metrics: the coefficient of determination (R^2), root mean square error (RMSE), and reduced chi-square (χ^2). These were computed using Eq. (4)-(6), as detailed below [18]:

$$\mathrm{R^2} = 1 - \left[\frac{\sum_{\mathrm{i=1}}^{\mathrm{N}} (\mathrm{MR_{pre,i}} - \mathrm{MR_{exp,i}})^2}{\sum_{\mathrm{i=1}}^{\mathrm{N}} (\overline{\mathrm{MR}}_{\mathrm{pre,i}} - \mathrm{MR_{exp,i}})^2}\right] \quad (4)$$

$$\mathrm{RMSE} = \left[\frac{1}{\mathrm{N}}\sum_{\mathrm{i=1}}^{\mathrm{N}} (\mathrm{MR_{exp,i}} - \mathrm{MR_{pre,i}})^2\right]^{1/2} \quad (5)$$

$$\chi^2 = \frac{\sum_{\mathrm{i=1}}^{\mathrm{N}} (\mathrm{MR_{exp,i}} - \mathrm{MR_{pre,i}})^2}{\mathrm{N} - \mathrm{z}} \quad (6)$$

where N was the number of observations, z was the number of constants, $MR_{exp,i}$ and $MR_{pre,i}$ were experimental and predicted moisture ratio, respectively. The optimal drying kinetics model was identified based on the highest average R^2 value, as well as the lowest average values for both χ^2 and RMSE.

Table 1 Mathematical models tested for tamarind foam-mat drying using far-infrared radiation combined with belt conveyor system in this study

Model name	Expression of moisture ratio (MR)	Reference
Newton	MR = exp(-kt)	[22]
Wang and Singh	MR = 1 + at + bt^2	[23]
Henderson and Pabis	MR = a exp(-kt)	[24]
Logarithmic	MR = a exp(-kt) + c	[25]
Verma et al.	MR = a exp(-kt) + (1-a) exp(-gt)	[26]
Two-term	MR = a exp(-kt) + b exp(-k_1t)	[27]
Midilli et al.	MR = a exp(-kt^n) + bt	[28]

2.8 Effective moisture diffusivity

The mathematical framework known as the diffusion model, rooted in Fick's second law, proves to be an invaluable tool for elucidating the rate at which moisture diffuses within a product during the drying process. When considering a finite slab undergoing the drying process, the formulation of Fick's second law can be expressed as [10]:

$$MR = \frac{8}{\pi^2}\exp(-\frac{\pi^2 D_{eff} t}{4L^2}) \quad (7)$$

By taking the natural logarithm of Eq. (7), a linear equation in the form of y = c + ax was obtained, where the variables were related as follows:

$$\ln MR = \ln\frac{8}{\pi^2} + (-\frac{\pi^2 D_{eff}}{4L^2})t \quad (8)$$

where MR was the moisture ratio (-), D_{eff} was the effective moisture diffusivity (m^2/s), t was the drying time (s) and L was the thickness of the tamarind foam-mat (m).

The calculation of the effective moisture diffusivity (D_{eff}) for tamarind foam-mats was performed using the slope method. This method is expressed as follows:

$$D_{eff} = -\frac{4aL^2}{\pi^2} \quad (9)$$

where D_{eff} was the effective moisture diffusivity (m^2/s), a was the slope of the plot of ln (MR) as a function of time (t) in Eq. (8), and L was the thickness of the tamarind foam-mat (m).

2.9 Statistical analysis

The analysis of data was carried out utilizing SPSS version 28 software. Initially, a one-way analysis of variance (ANOVA) was conducted, followed by Duncan's multiple tests, in order to detect noteworthy distinctions among tamarind foam-mat samples subjected to various drying conditions. All statistical examinations maintained a significance threshold of $P < 0.05$. To estimate parameters within the mathematical models of drying, non-linear regression analysis was applied, and the adequacy of these models was assessed using SPSS software.

3. Results and discussion

3.1 Drying kinetics of tamarind foam-mats

3.1.1 Effect of FIR power level on drying kinetics

The drying curves of tamarind foam-mats (TFMs), dried using far-infrared radiation (FIR) power levels of 400, 500, and 600 W, are shown in Figure 2. It was found that drying TFMs at higher FIR power levels led to a more rapid reduction in moisture content, resulting in shorter drying times compared to those dried at lower FIR power levels. This was because, as the FIR power level increased, more energy was delivered to the product, leading to higher internal temperatures within it. The elevated temperature differential between the interior and surface of the product accelerated the water vaporization process, promoting efficient moisture migration from the inside out. Consequently, the increased FIR power level expedited the evaporation process, reducing the time required to reach the desired moisture content. The results of this research were consistent with those of Adak et al. [29], who studied the effect of different infrared power levels (100, 200, and 300 W) on the drying kinetics of strawberries during combined infrared radiation and hot air drying. They observed that the drying time decreased with an increase in the infrared power level. They also noted that when using infrared power levels of 100, 200, and 300 W, the moisture content of the strawberries decreased from 91.80% w.b. to 10% w.b. within 440, 410, and 347 min, respectively. Another study by Silva et al. [11] investigated the influence of drying temperature (50, 60, 70, and 80°C) on the drying kinetics of TFMs during hot air drying. They found that the drying time decreased with an increase in the drying temperature. They also observed that the drying time of TFMs at a temperature of 50°C was 1.7 times greater than that at 80°C. Similarly, the findings of Sa-adchom et al. [16], which examined the effect of drying temperature (60, 70, and 80°C) on the drying kinetics of TFMs during FIR drying. They found that as the drying temperature increased, the vapor pressure gradient between the product's surface and the surrounding environment also increased, leading to enhanced moisture diffusion and evaporation rates. However, the effect of the FIR power level on drying kinetics of TFMs has not been previously reviewed in the literature.

3.1.2 Effect of thickness of tamarind foam-mats on drying kinetics

The drying curves of tamarind foam-mats (TFMs), with thicknesses of 3 and 6 mm, dried using a far infrared dryer combined with a belt conveyor system, are shown in Figure 3. It was observed that an increase in the thickness of the TFMs resulted in a slower reduction in moisture content and an extended drying time. This was because of the enhanced barrier to mass transfer within the material. When the thickness was increased, the distance that moisture had to travel to escape the foam-mat became greater, slowing down the diffusion of water molecules towards the surface. This made the internal moisture more trapped within the matrix of the foam, reducing the evaporation rate. Furthermore, the increased thickness likely led to a more uneven temperature distribution throughout the foam-mat, as the heat took longer to penetrate to the inner core of the material. This could cause a gradient in moisture content, with the outer layers drying faster than the inner ones, leading to a more time-consuming drying process overall. Consequently, the thicker TFMs exhibited reduced efficiency in drying, requiring more time to achieve the desired moisture reduction. This finding was in agreement with earlier studies conducted by Kandasamy et al. [8]. They investigated the effect of foam thickness (2, 4, 6, and 8 mm) on the drying characteristics of foamed papaya pulps in a batch-type cabinet tray dryer. They found that the drying time increased with the increase in foam thickness, because moisture migration was higher in areas with less foam thickness than in those with greater foam thickness. In addition, Dehghannya et al. [7] analyzed the effects of foam thickness (0.004, 0.005, and 0.006 m) on the drying kinetics of lime juice foam-mats during hot air drying. They observed that the rate of moisture content reduction slowed down with an increase in foam thickness.

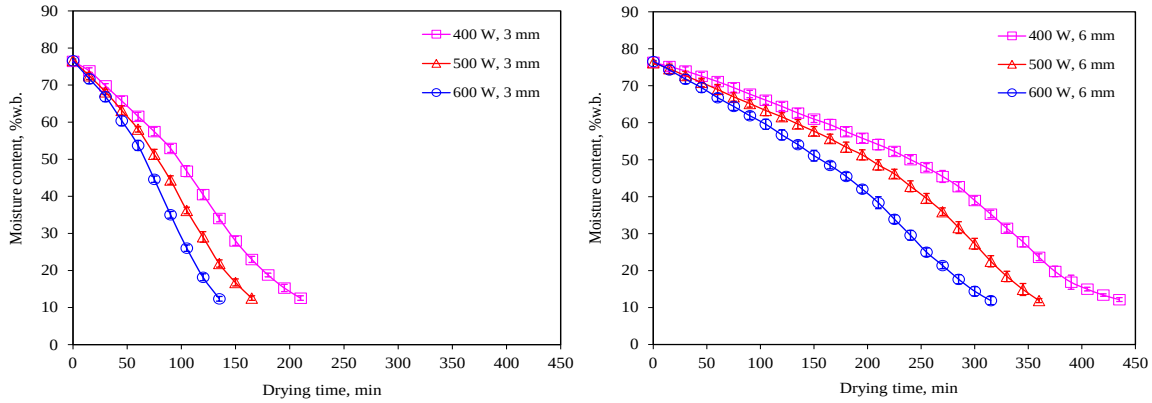

(a) Foam-mats with a thickness of 3 mm (b) Foam-mats with a thickness of 6 mm

Figure 2 Drying curves of tamarind foam-mats dried using far-infrared radiation power levels of 400, 500, and 600 W

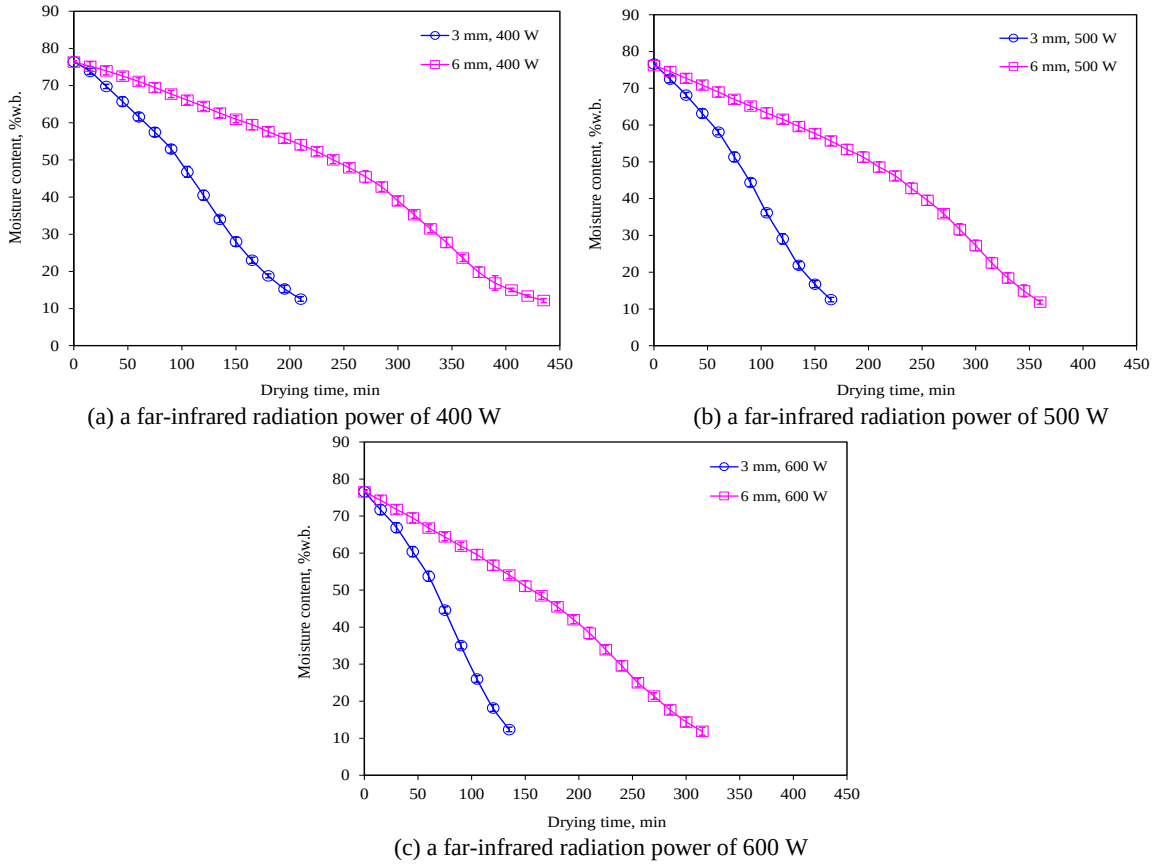

(a) a far-infrared radiation power of 400 W (b) a far-infrared radiation power of 500 W

(c) a far-infrared radiation power of 600 W

Figure 3 Drying curves of tamarind foam-mats with thicknesses of 3 and 6 mm, dried using a far-infrared dryer combined with a belt conveyor system

3.2 Specific energy consumption of tamarind foam-mat drying

3.2.1 Effect of FIR power level on specific energy consumption

The specific energy consumption (SEC) of tamarind foam-mat drying is presented in Table 2. It was observed that at the same thickness of tamarind foam-mats (TFMs), SEC significantly decreased with an increase in far-infrared radiation (FIR) power level. This occurred due to the higher power level of the FIR, resulting in a greater amount of energy being transferred to the product. Consequently, this led to an increase in internal temperatures within the product, enhancing heat transfer and moisture vaporization. As a result, the drying time was reduced, thereby lowering the overall energy required for the drying process. The findings of this research were in alignment with the work of Abbaspour-Gilandeh et al. [30]. They studied the influence of infrared power levels (250, 500, and 750 W) on the SEC of terebinth drying using an infrared dryer and found that as the infrared power level increased, the SEC decreased for all pretreatments. This occurred because the rise in infrared power level enhanced the moisture removal rate and shortened the drying time due to the thermal gradient between the product and the drying temperature. As a result, the efficiency of the process was increased. Another study by Kumar et al. [10] investigated the SEC of mango foam-mat drying using a convective hot-air dryer at temperatures of 60, 70, and 80°C. They observed that as the drying air temperature was increased, the SEC decreased. This reduction in SEC was attributed to the higher drying temperature, which led to a decrease in drying time and consequently, a reduction in energy consumption during drying. However, previous literature has not assessed the effect of varying FIR power levels on the specific energy consumption of TFMs.

Table 2 Specific energy consumption (SEC) of tamarind foam-mat drying

Thickness of foam-mat (mm)	FIR power (W)	Drying time (min)	SEC (MJ/kg_{water})
3	400	210	46.83 ± 0.22^{c}
	500	165	43.13 ± 0.21^{d}
	600	135	39.86 ± 0.23^{e}
6	400	435	48.99 ± 0.50^{a}
	500	360	48.09 ± 0.52^{b}
	600	315	46.98 ± 0.51^{c}

Values are presented as mean ± standard deviation. In the same column, different letter superscripts (a-e) indicate significant differences based on Duncan's multiple range test at $P < 0.05$.

3.2.2 Effect of thickness of tamarind foam-mats on specific energy consumption

In Table 2, it was observed that at the same FIR power level, increasing the thickness of tamarind foam-mats (TFMs) resulted in a significant increase in specific energy consumption (SEC). This was because, as the foam-mat thickness increased, the distance that heat and moisture had to traverse to reach the surface also increased, resulting in a longer diffusion path. Consequently, more energy was required to maintain efficient heat transfer and moisture removal throughout the thicker foam-mats. This increased energy requirement was a result of the necessity to overcome the resistance caused by the greater thickness. As a result, there was a significant increase in the SEC during the drying of TFMs. The findings of this study were consistent with those of Thanimkarn et al. [31], who examined the effects of different *Cissus quadrangularis* Linn. thicknesses (5, 10, and 15 mm) on the SEC during the infrared drying process. They observed that the thickest slice sample had the highest SEC, while the thinnest slice sample had the lowest SEC. This can be attributed to the increased energy required to transfer heat to the internal parts of the thicker slices due to the greater distance for heat transfer. Similarly, the findings of Hafezi et al. [32] investigated the effect of potato slice thicknesses (1, 2, and 3 mm) on the SEC during the vacuum-infrared method and concluded that as the slice thickness decreased, the SEC was reduced.

3.3 Colors of dried tamarind foam-mats and tamarind powder

3.3.1 Effect of FIR power level on the colors of dried tamarind foam-mats and tamarind powder

The colors of dried tamarind foam-mats (TFMs) are shown in Table 3. It was found that, at the same thickness, TFMs dried at a far-infrared radiation (FIR) power level of 600 W had significantly lower lightness (L^* value) and yellowness (b^* value), but higher redness (a^* value) and color difference (ΔE value), than those dried at an FIR power level of 400 W. This was due to the higher energy input accelerating moisture evaporation, leading to more pronounced Maillard reactions, which caused browning and darkening of the product. However, drying using an FIR power level of 500 W did not yield significantly different color values (L^*, a^*, b^*, and ΔE values) in dried TFMs when compared to those dried at FIR power levels of 400 and 600 W. This could indicate an optimal range of power levels within which the drying process did not significantly affect the color characteristics. The FIR power level of 500 W might have fallen within this optimal region, allowing for a balance between drying efficiency and the retention of color properties. The results of this study were in agreement with those of Amini et al. [19], Doymaz [33], and Salehi and Satorabi [34], who found that an increase in the FIR power level led to a rise in the darkness-brownness of agricultural products and resulted in pigment destruction. This was because as the FIR power level increased, there was a corresponding increase in internal temperatures within the product, leading to more Maillard reactions. Another study by Sa-adchom et al. [16] examined the drying of tamarind foam-mats (TFMs) using FIR at drying temperatures of 60, 70, and 80°C. They found that the TFMs dried at lower temperatures exhibited higher lightness (L^* value) and yellowness (b^* value), but lower redness (a^* value), compared to those dried at higher temperatures.

The colors of tamarind powder are shown in Table 4. It was found that, at the same thickness, tamarind powder with FIR power levels of 400, 500, and 600 W were not significantly different in color values (L^*, a^*, b^*, and ΔE values). This was because the effect of FIR primarily influenced the browning on the surface of the product. Consequently, when the product was ground into a powder, the internal color became apparent. As a result, tamarind powder produced from TFMs dried using FIR at 400, 500, and 600 W exhibited similar colors. The findings of this study were similar to those of Ekpong et al. [12], who examined the effects of drying temperatures

(55, 60, and 70°C) on the color of dried tamarind powder. They found that no significant difference in the color values (*L**, *a**, and *b** values) of the powder samples when the drying temperature increased from 55 to 70°C at a constant maltodextrin content. Similarly, the results of Silva et al. [11], which dried TFMs using hot air drying. They found that tamarind powder with hot air temperatures of 50, 70, and 80°C were not significantly different in lightness (*L** value), while tamarind powder with hot air temperatures of 60 and 70°C were not significantly different in hue (h^o value). However, the impact of different power levels of FIR on the color of tamarind powder has not been examined in earlier studies.

Table 3 Colors of dried tamarind foam-mats

Thickness of foam-mat (mm)	FIR power (W)	Drying time (min)	Colors			
			L*	***a****	***b****	**Δ*E***
3	400	210	21.90±0.86^{a}	4.74±0.39^{c}	36.63±0.96^{a}	13.12±1.21^{d}
	500	165	20.64±0.89^{ab}	5.14±0.44^{bc}	35.52±1.06^{ab}	14.73±1.40^{cd}
	600	135	19.45±0.70^{bc}	5.65±0.41^{ab}	34.01±1.16^{b}	16.69±1.31^{c}
6	400	435	18.37±0.66^{cd}	5.36±0.40^{bc}	31.85±0.68^{c}	19.06±0.60^{b}
	500	360	17.41±0.61^{de}	5.81±0.37^{ab}	30.54±0.83^{cd}	20.70±0.97^{ab}
	600	315	16.51±0.77^{e}	6.22±0.42^{a}	29.30±0.81^{d}	22.26±1.14^{a}

Values are presented as mean ± standard deviation. In the same column, different letter superscripts (a-e) indicate significant differences based on Duncan's multiple range test at $P < 0.05$.

Table 4 Colors of tamarind powder

Thickness of foam-mat (mm)	FIR power (W)	Drying time (min)	Colors			
			L*	***a****	***b****	**Δ*E***
3	400	210	22.64±0.38^{b}	4.35±0.27^{abc}	38.48±0.37^{b}	11.11±0.26^{a}
	500	165	22.57±0.37^{b}	4.49±0.22^{ab}	38.90±0.23^{b}	10.79±0.29^{a}
	600	135	22.45±0.42^{b}	4.67±0.20^{a}	38.77±0.37^{b}	10.99±0.28^{a}
6	400	435	26.10±0.37^{a}	3.92±0.20^{d}	46.73±0.40^{a}	2.42±0.49^{b}
	500	360	25.94±0.36^{a}	4.05±0.25^{cd}	46.09±0.42^{a}	3.00±0.46^{b}
	600	315	26.21±0.39^{a}	4.20±0.19^{bcd}	46.38±0.41^{a}	2.68±0.17^{b}

Values are presented as mean ± standard deviation. In the same column, different letter superscripts (a-d) indicate significant differences based on Duncan's multiple range test at $P < 0.05$.

3.3.2 Effect of thickness of tamarind foam-mats on the colors of dried tamarind foam-mats and tamarind powder

In Table 3, it was found that at the same far-infrared radiation (FIR) power level, the 6 mm thick tamarind foam-mats (TFMs) had significantly lower lightness (*L** value) and yellowness (*b** value), but higher color differences (Δ*E* value) than the 3 mm thick ones. This was due to the fact that the 6 mm thick TFMs required longer drying times, causing the product to be heated for an extended period. As a result, the Maillard reactions occurred more prominently in the 6 mm thick TFMs compared to the 3 mm thick ones. However, when drying the TFMs with thicknesses of 3 and 6 mm, the redness value, as indicated by the *a** value, was found to be not significantly different between the two samples. This lack of significant difference might be attributed to the nature of the drying process and the specific properties of tamarind itself. The color parameter *a**, which represents redness, is likely more influenced by factors such as the intrinsic pigmentation of tamarind, temperature, drying method, and FIR power level, rather than by the thickness of the foam-mats. The findings of this study were in agreement with those of Zhang et al. [35], Wu et al. [36], and Jafari et al. [37]. They found that in FIR drying, the thicknesses of products affected the color values (*L**, *a**, and *b** value) of the products. This effect was due to non-enzymatic browning reactions like the Maillard reaction, which proceeded to a higher degree in thicker pieces compared to thinner ones.

In Table 4, it showed that at the same FIR level, tamarind powder produced from 6 mm thick TFMs had significantly higher lightness (*L** value) and yellowness (*b** value), but lower redness (*a** value) than those of 3 mm thick TFMs This was due to the high quantity of pulp within the 6 mm thick TFMs. Consequently, when the grinding process was used to produce powdered tamarind, the inner pulp's color became more pronounced in the final product than in the case of the 3 mm thick TFMs. The results of this study were similar to those of Salahi et al. [9] and Hamzeh et al. [38]. They found that the thickness of the foam mats affected the color values of the product powders. However, previous studies have not investigated the effect of the thickness of TFMs on the colors of tamarind powder.

3.4 Dissolution time of tamarind powder

The test for dissolution time evaluates the capability to fully reconstitute powder in water. A shorter time required for dissolution indicates a higher quality of the powder. The dissolution times of tamarind powder were shown in Table 5. It was found that, at the same thickness, the dissolution time of tamarind powder significantly decreased with an increase in far-infrared radiation (FIR) power level. This occurred due to the increased power level of the FIR, which led to a greater supply of energy to the product. As a consequence, the internal temperatures were raised. The greater temperature difference between the product's interior and its surface caused rapid evaporation of moisture from the foam-mat structure. This resulted in the foam-mat having an amorphous structure and a more porous [9], which enlarged its surface area and shortened the diffusion distance for water molecules during dissolution testing. The findings of this study were similar to those of Salahi et al. [9], who investigated the effect of different drying temperatures (40, 55, and 70°C) on the dissolution time of foam-mat-dried cantaloupe pulp powder. They found that as the drying temperature increased, the reconstitution speed of the powder into water also increased, and therefore the dissolution time decreased. In scanning electron micrographs, they observed that the dried foam-mats exhibited a more porous appearance at higher drying temperatures, indicating increased porosity within these dried foam-mats. As the porosity increased, the greater specific surface area led to a reduction in the time required for dissolution.

In Table 5, it was found that at the same FIR power level, the dissolution time of tamarind powder significantly increased with an increase in the thickness of tamarind foam-mats. This was because as the thickness of the foam-mats increased, the drying time was prolonged, leading to a change in the microstructure and porosity of the material. This often led to a more compact and less porous structure. Consequently, when the dried tamarind powder was mixed with water, the water molecules had a more difficult time penetrating the compacted structure, resulting in a slower dissolution process. The findings were consistent with previous research conducted by Salahi et al. [9], which investigated the effect of different thicknesses (3 and 5 mm) on the dissolution time of foam-mat-dried cantaloupe pulp powder. They found that increasing the thickness of cantaloupe pulp foam mats from 3 to 5 mm led to a prolonged dissolution period, especially at a temperature of 40°C. The scanning electron micrographs showed that as the thickness of the dried foam-mats decreased, the dried foam-mats retained their structure and became more porous. This led to a greater specific surface area, resulting in a decreased dissolution time of cantaloupe pulp powder. Similarly, Abd El-Salam et al. [39] studied the effect of different thicknesses of papaya pulp foam-mats (2, 4, and 6 mm) on the dissolution time of papaya pulp powder and reported that increasing the thickness of papaya pulp foam-mats from 2 to 6 mm resulted in a longer dissolution time for papaya pulp powder.

Table 5 Dissolution times of tamarind powder

Thickness of foam-mat (mm)	FIR power (W)	Drying time (min)	Dissolution time (s)
3	400	210	70.70 ± 4.83^{b}
	500	165	56.52 ± 5.13^{c}
	600	135	39.69 ± 4.32^{d}
6	400	435	96.42 ± 4.21^{a}
	500	360	78.59 ± 4.69^{b}
	600	315	57.93 ± 5.09^{c}

Values are presented as mean ± standard deviation. In the same column, different letter superscripts (a-d) indicate significant differences based on Duncan's multiple range test at $P < 0.05$.

3.5 Evaluation of the drying models

The moisture content data collected under different drying conditions were transformed into moisture ratio expressions and used regression analysis to fit curves with drying time using the seven drying models listed in Table 1. The drying coefficients (a, b, c, g, k and k_1) obtained from these models, along with statistical analyses evaluating the models' performance under various drying conditions, such as the coefficient of determination (R^2), root mean square error (RMSE), and reduced chi-square (χ^2), are presented in Tables 6 and 7 for tamarind foam-mats with a thickness of 3 and 6 mm, respectively.

Table 6 Prediction of model coefficients for tamarind foam-mats with a thickness of 3 mm

Model	FIR power (W)	Constants				R^2	RMSE	χ^2
Newton [22]		k						
	400	0.012150				0.993525	0.017209	0.00027023
	500	0.015051				0.992271	0.019128	0.00032846
	600	0.017734				0.989605	0.025321	0.00045215
		Average				0.991800	0.020553	0.00035028
Wang and Singh [23]		a	b					
	400	-0.009239	0.000022			0.999204	0.008670	0.00000893
	500	-0.011421	0.000034			0.999242	0.008023	0.00000339
	600	-0.013854	0.000051			0.998752	0.013582	0.00003928
		Average				0.999066	0.010092	0.00001720
Henderson and Pabis [24]		a	k					
	400	1.065200	0.012935			0.990881	0.005861	0.00007486
	500	1.058280	0.015915			0.989642	0.008845	0.00014034
	600	1.059850	0.018772			0.986544	0.014781	0.00024266
		Average				0.989022	0.009829	0.00015262
Logarithmic [25]		a	k	c				
	400	1.160740	0.009935	-0.125222		0.996834	0.006515	0.00002540
	500	1.177000	0.011789	-0.148421		0.996856	0.007609	0.00002846
	600	1.218200	0.013102	-0.189398		0.996083	0.011087	0.00003083
		Average				0.996591	0.008403	0.00002823
Verma et al. [26]		a	k	g				
	400	-245.472000	0.021619	0.021562		0.999188	0.006548	0.00001130
	500	45.006900	0.007581	0.007479		0.996998	0.009033	0.00000171
	600	-302.426000	0.035634	0.035589		0.966518	0.043753	0.00370168
		Average				0.987568	0.019778	0.00123823
Two-term [27]		a	k	b	k_1			
	400	-17.842100	0.005033	18.844000	0.005225	0.993505	0.005446	0.00002020
	500	-28.305000	0.003407	29.306800	0.003603	0.981163	0.001660	0.00037748
	600	-28.696300	0.003195	29.700100	0.003446	0.965770	0.043759	0.00431985
		Average				0.980146	0.016955	0.00157251
Midilli et al. [28]		a	k	n	b			
	400	1.003950	0.003927	1.247740	-0.000030	0.999759	0.001496	0.00000725
	500	0.990011	0.004338	1.282440	-0.000047	0.999687	0.001168	0.00001058
	600	1.001800	0.005073	1.297120	-0.000094	0.999832	0.000893	0.00001395
		Average				0.999759	0.001186	0.00001059

Table 7 Prediction of model coefficients for tamarind foam-mats with a thickness of 6 mm

Model	FIR power (W)	Constants				R^2	RMSE	χ^2
		k						
Newton [22]	400	0.005200				0.990093	0.002624	0.00002279
	500	0.006176				0.988988	0.002852	0.00000202
	600	0.007991				0.995335	0.000439	0.00000282
	Average					0.991472	0.001972	0.00000921
		a	b					
Wang and Singh [23]	400	-0.003920	0.000004			0.997186	0.000503	0.00000079
	500	-0.004734	0.000006			0.994145	0.006613	0.00006758
	600	-0.006135	0.000010			0.993402	0.005388	0.00010544
	Average					0.994911	0.004168	0.00005794
		a	k					
Henderson and Pabis [24]	400	1.045770	0.005452			0.987595	0.004436	0.00000160
	500	1.010080	0.006244			0.988457	0.004503	0.00000809
	600	1.006270	0.008044			0.995116	0.001474	0.00000647
	Average					0.990389	0.003471	0.00000538
		a	k	c				
Logarithmic [25]	400	1.245330	0.003441	-0.250053		0.998603	0.001227	0.00000246
	500	1.205810	0.003990	-0.240656		0.997791	0.000431	0.00000124
	600	1.078710	0.006421	-0.099489		0.998629	0.001026	0.00000645
	Average					0.998341	0.000895	0.00000338
		a	k	g				
Verma et al. [26]	400	26.251900	0.007832	0.007962		0.992042	0.001172	0.00000618
	500	5.490390	0.007361	0.007486		0.983552	0.001156	0.00000328
	600	12.540800	0.009818	0.009982		0.995119	0.000531	0.00000321
	Average					0.990237	0.000953	0.00000422
		a	k	b	k_1			
Two-term [27]	400	26.567100	0.007805	-25.559600	0.007933	0.991967	0.000045	0.00000186
	500	12.747500	0.009247	-11.745200	0.009387	0.973904	0.000669	0.00003509
	600	26.518800	0.012388	-25.515400	0.012569	0.992599	0.001224	0.00000367
	Average					0.986156	0.000646	0.00001354
		a	k	n	b			
Midilli et al. [28]	400	1.032810	0.007596	0.877179	-0.000450	0.998534	0.001040	0.00000133
	500	1.032100	0.018092	0.712479	-0.000784	0.999234	0.000440	0.00000165
	600	1.037460	0.017036	0.810131	-0.000452	0.999086	0.000280	0.00000005
	Average					0.998951	0.000587	0.00000101

In Tables 6 and 7, the statistical analysis was conducted on several models, which yielded varying values of coefficient of determination (R^2), root mean square error (RMSE), and reduced chi-square (χ^2). The decision criteria for selecting the best model involved a comprehensive analysis of these statistical indicators. A high value of R^2 indicated a good fit to the experimental data, while the low values of RMSE and χ^2 provided information about the magnitude of the residuals and the goodness of fit, respectively.

In Table 6, for the tamarind foam-mats (TFMs) with a 3 mm thickness, the Midilli et al. model yielded the highest average value of R^2 (0.999759) and the lowest average values for RMSE (0.001186) and χ^2 (0.00001059). In Table 7, for the TFMs with a 6 mm thickness, the Midilli et al. model produced the highest average value of R^2 (0.998951) and the lowest average values for RMSE (0.000587) and χ^2 (0.00000101). Therefore, the Midilli et al. model was selected to describe the drying characteristics of TFMs undergoing far-infrared radiation drying combined with a belt conveyor system. The result was consistent with prior research on the drying process of TFMs, as reported by Silva et al. [11]. They investigated a mathematical model to describe the drying behavior of TFMs and found that the Midilli et al. model was in good agreement with the experimental results, with an R^2 value ranging from 0.9978 to 0.9989 and an RMSE value between 0.01064 and 0.01612.

The selected model's validity was verified by comparing the predicted moisture ratio to the experimental moisture ratio under various drying conditions. Figure 4 displays comparisons between the experimental and predicted moisture ratios against drying time, demonstrating that the Midilli et al. model aligns well with the experimental outcomes. In addition, the plot of predicted moisture ratio versus experimental moisture ratio, as shown in Figure 4, appeared as a straight line, indicating that the Midilli et al. model accurately described the drying behavior of the TFMs.

Based on the above analysis, in order to use the Midilli et al. model to calculate the moisture ratio of tamarind foam-mats (TFMs) within the ranges of FIR power levels (400, 500, and 600 W) and the thicknesses of TFMs (3 and 6 mm) in this study, it was necessary to consider the constant values of a, k, n, and b in the Midilli et al. model as a non-linear equation in terms of the FIR power level (E) and the thickness of TFMs (T). This non-linear equation was expressed as:

$$a = x_0 + x_1E + x_2T \quad (10)$$

$$k = x_3 + x_4E + x_5T \quad (11)$$

$$n = x_6 + x_7E + x_8T \quad (12)$$

$$b = x_9 + x_{10}E + x_{11}T \quad (13)$$

where a, k, n, b, x_0 to x_{11} were constant values, E was the FIR power level (W), and T was the thickness of TFMs (mm). Therefore, the Midilli et al. model could be expressed in the form of Eq. (14), as shown below:

$$MR = (x_0 + x_1E + x_2T)\exp(-(x_3 + x_4E + x_5T)t^{(x6 + x7E + x8T)}) + (x_9 + x_{10}E + x_{11}T)t \quad (14)$$

where MR was the moisture ratio (-), and t was the drying time (min). Eq. (14) was analyzed using regression analysis to determine the constant values of the equation. The results of the analysis were presented in Eq. (15), which could be used to explain the drying behavior of TFMs at FIR power levels of 400, 500, and 600 W and with thicknesses of 3 and 6 mm.

$$MR = a\exp(-kt^n) + bt \quad (15)$$

where $a = 0.959926 + 6.25\times10^{-6}E + 0.0118454T$, $k = -0.0185816 + 2.64648\times10^{-5}E + 0.00326503T$, $n = 1.77369 - 4.417\times10^{-5}E - 0.158612T$, and $b = 0.000530438 - 1.64453\times10^{-7}E - 0.000168316T$. The analysis of the Midilli et al. model in Eq. (15) resulted in an R^2 value of 0.993269, an RMSE of 0.005117, and a χ^2 value of 0.000321. These outcomes indicated that the model was suitable for describing the drying behavior of TFMs.

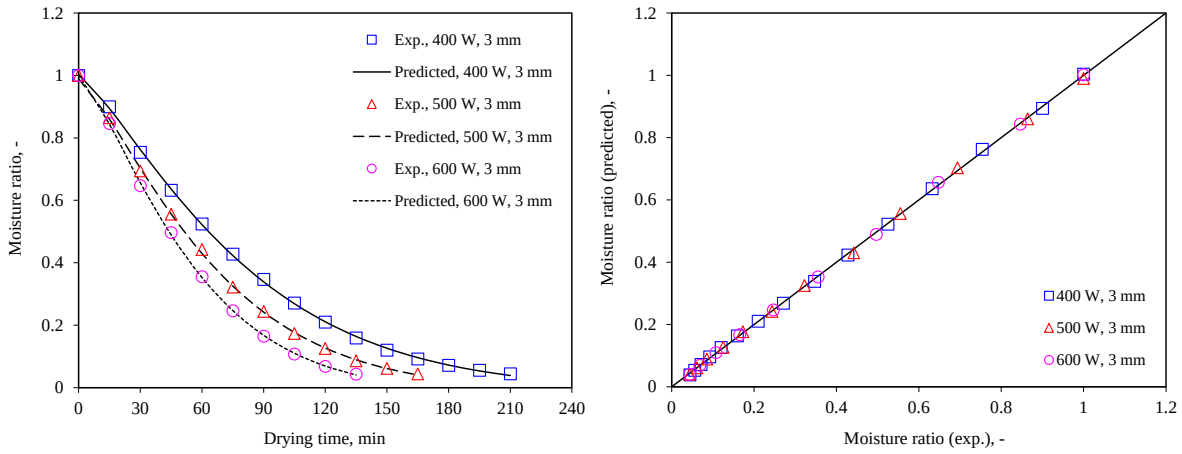

(a) tamarind foam-mats with a 3 mm thickness

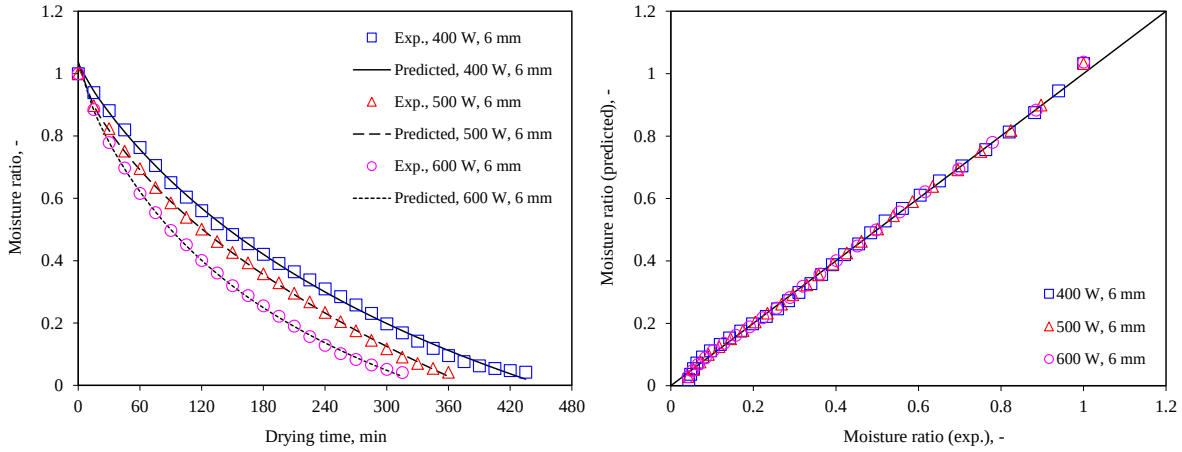

(b) tamarind foam-mats with a 6 mm thickness

Figure 4 Comparisons between experimental data and best fit of Midilli et al. model at FIR power levels of 400, 500, and 600 W

3.6 Effective moisture diffusivity

The effective moisture diffusivity (D_{eff}) values of tamarind foam-mats (TFMs) for different drying conditions are presented in Table 8. It was observed that increasing the FIR power level resulted in an increase in the D_{eff} value of TFMs. This was because, as the FIR power level increased, the product absorbed more energy, which led to higher internal temperatures within it. This elevated temperature created a steeper gradient between the surfaces and interiors of the foam-mats, causing faster moisture evaporation from the surfaces. This rapid evaporation, driven by the increased thermal energy, enhanced the diffusion of moisture from the interior to the surface, ultimately resulting in a higher D_{eff} value. The results of this study were similar to those of Diógenes et al. [40], who found that higher temperatures resulted in an increase in the D_{eff} values of cumbeba pulp foam-mats. This was because the rise in temperature led to an enhanced heat transfer rate between the foam and the drying air, resulting in greater agitation of water molecules and increased diffusion. The D_{eff} values of cumbeba pulp foam-mats ranged from 1.037×10^{-9} to 6.103×10^{-9} m^2/s. Similarly, the findings of Branco et al. [41] found that the D_{eff} values of uvaia pulp foam-mats increased with the increasing drying temperature, due to accelerated water removal at higher temperatures. For uvaia pulp foam-mats, the D_{eff} values ranged from 6.41×10^{-10} and 8.95×10^{-10} m^2/s.

In Table 8, it was observed that the D_{eff} value increased with the thickness of the TFMs. This was because as the TFMs became thicker, more pathways became available for moisture movement, thereby reducing the resistance to moisture diffusion. Consequently, this led to a more efficient transfer of moisture through the TFMs, resulting in an increase in the D_{eff} value. This finding concurred

with the results reported by Kamali et al. [21], who observed that the D_{eff} value increased with an increase in the thickness of banana foam-mats. This was because, at higher foam thicknesses, the internal moisture transfer occurred along a longer distance than at lower foam thicknesses. For banana foam-mats, the D_{eff} values ranged between 2.397×10^{-9} and 6.792×10^{-9} m^2/s. Similarly, the results of Osama et al. [42] found that the D_{eff} value increased with the increasing thickness of kadam pulp foam-mats. This was due to the fact that D_{eff} is proportional to the square of the foam thickness, resulting in an increase in the foam thickness that led to an increase in the D_{eff} value. The D_{eff} values of kadam pulp foam-mats were in the range of 4.96×10^{-10} to 4.23×10^{-9} m^2/s. However, the D_{eff} value of tamarind foam-mats (TFMs) has not been previously reviewed in the literature. It should be noted the D_{eff} values of TFMs obtained in this study (9.41×10^{-10} - 2.33×10^{-9} m^2/s) fall within a range similar to those of products in previous studies on foam-mat drying, as mentioned above.

Table 8 Effective moisture diffusivity value of tamarind foam-mats for each drying condition

Thickness of foam-mat (mm)	FIR power (W)	Effective moisture diffusivity value (m^2/s)
3	400	9.41×10^{-10}
	500	1.18×10^{-9}
	600	1.44×10^{-9}
6	400	1.72×10^{-9}
	500	1.93×10^{-9}
	600	2.33×10^{-9}

4. Conclusions

This research examined the impact of different power levels of far-infrared radiation (FIR) and the thickness of tamarind foam-mats (TFMs) on the drying kinetics, specific energy consumption, color, and dissolution time of tamarind powder. The experiment utilized FIR drying in conjunction with a belt conveyor system, with FIR power levels set at 400, 500, and 600 W, and TFMs thicknesses of 3 and 6 mm. The experimental results showed that higher FIR power levels resulted in quicker reductions in moisture content in TFMs, reduced SEC, and faster dissolution of tamarind powder in water, compared to lower FIR power levels. TFMs that were 3 mm thick exhibited a faster decrease in moisture content, lower SEC, and a more rapid dissolution of tamarind powder in water than the 6 mm thick ones. In addition, tamarind powder produced from TFMs that were 6 mm thick had a higher lightness (L^* value) and yellowness (b^* value), but lower redness (a^* value) than that produced from 3 mm thick TFMs. However, there were no significant differences in color values (L^*, a^*, and b^* values) for tamarind powder produced from TFMs at FIR power levels of 400, 500, and 600 W. The optimal condition for drying TFMs using a far-infrared dryer combined with a belt conveyor system was determined to be foam-mats with a thickness of 3 mm and an FIR power level of 600 W. This condition yielded the shortest drying time (135 min), the lowest SEC (39.86 ± 0.23 MJ/kg_{water}), the quickest dissolution of tamarind powder in water (39.69 ± 4.32 s), and color values of tamarind powder within an acceptable range ($L^* = 22.45\pm0.42$, $a^* = 4.67\pm0.20$, and $b^* = 38.77\pm0.37$). The statistical analysis revealed that the Midilli et al. model accurately represented the drying characteristics of TFMs using FIR combined with a belt conveyor system. This finding was supported by a high coefficient of determination (R^2) value of 0.993269, a low root mean square error (RMSE) value of 0.005117, and a small reduced chi-squared (χ^2) value of 0.000321. The effective moisture diffusivity values for TFMs ranged from 9.41×10^{-10} to 2.33×10^{-9} m^2/s. Additionally, this study highlighted several distinct advantages of using FIR in conjunction with a belt conveyor system for drying TFMs. The optimal FIR power level and foam-mat thickness were found to significantly enhance drying kinetics, resulting in reduced drying times and improved quality attributes such as color and dissolution time of tamarind powder. The mathematical model that was developed aided in predicting and optimizing the drying process, demonstrating potential for efficient and quality-focused industrial applications.

5. Acknowledgements

The author would like to express gratitude for the support and resources provided by the Faculty of Engineering at Rajamangala University of Technology Lanna.

6. References

[1] Uma Maheswari C, Obi Reddy K, Varada Rajulu A, Guduri BR. Tensile properties and thermal degradation parameters of tamarind fruit fibers. J Reinf Plast Compos. 2008;27(16-17):1827-32.
[2] Natukunda S, Muyonga JH, Mukisa IM. Effect of tamarind (*Tamarindus indica* L.) seed on antioxidant activity, phytocompounds, physicochemical characteristics, and sensory acceptability of enriched cookies and mango juice. Food Sci Nutr. 2015;4(4):494-507.
[3] Zhao R, Xiao H, Liu C, Wang H, Wu Y, Ben A, et al. Dynamic changes in volatile and non-volatile flavor compounds in lemon flavedo during freeze-drying and hot-air drying. LWT. 2023;175:114510.
[4] Qadri OS, Srivastava AK, Yousuf B. Trends in foam mat drying of foods: special emphasis on hybrid foam mat drying technology. Crit Rev Food Sci Nutr. 2020;60(10):1667-76.
[5] Reis FR, de Moraes ACS, Masson ML. Impact of foam-mat drying on plant-based foods bioactive compounds: a review. Plant Foods Hum Nutr. 2021;76(2):153-60.
[6] Hardy Z, Jideani VA. Foam-mat drying technology: a review. Crit Rev Food Sci Nutr. 2017;57(12):2560-72.
[7] Dehghannya J, Pourahmad M, Ghanbarzadeh B, Ghaffari H. Influence of foam thickness on production of lime juice powder during foam-mat drying: experimental and numerical investigation. Powder Technol. 2018;328:470-84.
[8] Kandasamy P, Varadharaju N, Kalemullah S, Maladhi D. Optimization of process parameters for foam-mat drying of papaya pulp. J Food Sci Technol. 2014;51(10):2526-34.

[9] Salahi MR, Mohebbi M, Taghizadeh M. Development of cantaloupe (*Cucumis melo*) pulp powder using foam-mat drying method: effects of drying conditions on microstructural of mat and physicochemical properties of powder. Dry Technol. 2017;35(15):1897-908.
[10] Kumar A, Kandasamy P, Chakraborty I, Hangshing L. Analysis of energy consumption, heat and mass transfer, drying kinetics and effective moisture diffusivity during foam-mat drying of mango in a convective hot-air dryer. Biosyst Eng. 2022;219:85-102.
[11] Silva AS, Gurjão KC de O, Almeida F de AC, Bruno R de LA, Pereira WE. Dehydration of tamarind pulp through the foam-mat drying method. Ciênc Agrotec. 2008;32(6):1899-905. (In Portuguese)
[12] Ekpong A, Phomkong W, Onsaard E. The effects of maltodextrin as a drying aid and drying temperature on production of tamarind powder and consumer acceptance of the powder. Int Food Res J. 2016;23(1):300-8.
[13] International Commission on Non-Ionizing Radiation Protection. ICNIRP statement on far infrared radiation exposure. Health Phys. 2006;91(6):630-45.
[14] Salehi F. Recent applications and potential of infrared dryer systems for drying various agricultural products: a review. Int J Fruit Sci. 2020;20(3):586-602.
[15] Nathakaranakule A, Jaiboon P, Soponronnarit S. Far-infrared radiation assisted drying of longan fruit. J Food Eng. 2010;100(4):662-8.
[16] Sa-adchom P, Supavititpatana P, Supawithitpattana T. Effect of drying temperature on foam-mat tamarind drying using far-infrared radiation. Proceedings of the 18th TSAE National Conference and the 10th TSAE International Conference; 2017 Sep 7-9; Bangkok, Thailand. Bangkok: TSAE; 2017. p. 277-82. (In Thai)
[17] Salehi F, Satorabi M. Influence of infrared drying on drying kinetics of apple slices coated with basil seed and xanthan gums. Int J Fruit Sci. 2021;21(1):519-27.
[18] Sa-adchom P. Drying kinetics and mathematical modeling of spent coffee grounds drying using the spouted bed technique. Eng Appl Sci Res. 2023;50(4):324-34.
[19] Amini G, Salehi F, Rasouli M. Color changes and drying kinetics modeling of basil seed mucilage during infrared drying process. Inf Process Agric. 2022;9(3):397-405.
[20] Al-Kahtani HA, Hassan BH. Spray drying of roselle (*Hibiscus sabdariffa* L.) extract. J Food Sci. 1990;55(4):1073-6.
[21] Kamali R, Dadashi S, Dehghannya J, Ghaffari H. Numerical simulation and experimental investigation of foam-mat drying for producing banana powder as influenced by foam thickness. Appl Food Res. 2022;2(1):100075.
[22] Lewis WK. The rate of drying of solid materials. Ind Eng Chem. 1921;13(5):427-32.
[23] Wang CY, Singh RP. A single layer drying equation for rough rice (ASAE Paper No: 78-3001). Michigan: ASAE; 1978.
[24] Henderson SM, Pabis S. Grain drying theory I. Temperature effect on drying coefficient. J Agric Eng Res. 1961;6:169-74.
[25] Toğrul İT, Pehlivan D. Mathematical modelling of solar drying of apricots in thin layers. J Food Eng. 2002;55(3):209-16.
[26] Verma LR, Bucklin RA, Endan JB, Wratten FT. Effects of drying air parameters on rice drying models. Trans ASAE. 1985;28(1):0296-0301.
[27] Henderson SM. Progress in developing the thin layer drying equation. Trans ASAE. 1974;17(6):1167-8.
[28] Midilli A, Kucuk H, Yapar Z. A new model for single-layer drying. Dry Technol. 2002;20(7):1503-13.
[29] Adak N, Heybeli N, Ertekin C. Infrared drying of strawberry. Food Chem. 2017;219:109-16.
[30] Abbaspour-Gilandeh Y, Kaveh M, Fatemi H, Khalife E, Witrowa-Rajchert D, Nowacka M. Effect of pretreatments on convective and infrared drying kinetics, energy consumption and quality of terebinth. Appl Sci. 2021;11(16):7672.
[31] Thanimkarn S, Cheevitsopon E, Jongyingcharoen JS. Effects of vibration, vacuum, and material thickness on infrared drying of *Cissus quadrangularis* Linn. Heliyon. 2019;5(6):e01999.
[32] Hafezi N, Sheikhdavoodi MJ, Sajadiye SM, Ferdavani MEK. Evaluation of energy consumption of potato slices drying using vacuum-infrared method. Int J Adv Biol Biomed Res. 2014;2(10):2651-8.
[33] Doymaz İ. Infrared drying kinetics and quality characteristics of carrot slices. J Food Process Preserv. 2015;39(6):2738-45.
[34] Salehi F, Satorabi M. Effect of basil seed and xanthan gums coating on colour and surface change kinetics of peach slices during infrared drying. Acta Technol Agric. 2021;24(3):150-6.
[35] Zhang L, Wang X, Yu L, Zhang H. Drying characteristics and color changes of infrared drying eggplant. TCSAE. 2012;28(S2):291-6.
[36] Wu B, Guo Y, Wang J, Pan Z, Ma H. Effect of thickness on non-fried potato chips subjected to infrared radiation blanching and drying. J Food Eng. 2018;237:249-55.
[37] Jafari F, Movagharnejad K, Sadeghi E. Infrared drying effects on the quality of eggplant slices and process optimization using response surface methodology. Food Chem. 2020;333:127423.
[38] Hamzeh S, Motamedzadegan A, Shahidi SA, Ahmadi M, Regenstein JM. Effects of drying condition on physico-chemical properties of foam-mat dried shrimp powder. J Aquat Food Prod Technol. 2019;28(7):794-805.
[39] Abd El-Salam EAES, Ali AM, Hammad KS. Foaming process optimization, drying kinetics and quality of foam mat dried papaya pulp. J Food Sci Technol. 2021;58:1449-61.
[40] Diógenes AMG, de Figueirêdo RMF, Queiroz AJM, Ferreira JPL, Silva WPD, Gomes JP, et al. Mathematical models to describe the foam mat drying process of cumbeba pulp (*Tacinga inamoena*) and product quality. Foods. 2022;11(12):1751.
[41] Branco IG, Kikuchi TT, Argandoña EJS, Moraes ICF, Haminiuk CWI. Drying kinetics and quality of uvaia (*Hexachlamys edulis* (O. Berg)) powder obtained by foam-mat drying. Int J Food Sci Technol. 2016;51(7):1703-10.
[42] Osama K, Younis K, Qadri OS, Parveen S, Siddiqui MH. Development of under-utilized kadam (*Neolamarkia cadamba*) powder using foam mat drying. LWT. 2022;154:112782.